ASIAN JOURNAL OF PHARMACEUTICAL AND CLINICAL RESEARCH

INNOVARE ACADEMIC SCIENCES
Knowledge to Innovation

Vol 18, Issue 11, 2025

Online - 2455-3891
Print - 0974-2441

Research Article

# MOLECULAR DOCKING, ADMET, SYNTHESIS, AND PRELIMINARY PHARMACOLOGICAL EVALUATION OF NEW ETODOLAC DERIVATIVES CONTAINING PYRAZOLINE MOIETY

**HASSAN F. ABED[1]*, TAGREED N-A OMAR[2]**

[1]Ministry of Health, Al-Qadisiya, Iraq. [2]Department of Pharmaceutical Chemistry, College of Pharmacy, University of Baghdad, Baghdad, Iraq.
*Corresponding author: Hassan F. Abed; Email: hasan.abd2200m@copharm.uobaghdad.edu.iq

*Received: 06 August 2025, Revised and Accepted: 16 September 2025*

**ABSTRACT**

**Objective:** The main objectives were to use molecular docking to create compounds with antibacterial activity and anti-inflammatory properties that are still effective. For future application, these compounds must also have acceptable absorption, distribution, metabolism, excretion, and possible toxicity (ADMET) characteristics.

**Methods:** Ligand Designer using Glide (Schrodinger LLC) molecular docking studies. A new etodolac derivative containing a pyrazoline ring was synthesized and characterized using ATR-FTIR and 1H-NMR. Furthermore, their pharmacological activities were investigated. In order to determine the derivatives' pharmacological characteristics, we used a rat model for anti-inflammatory activity called rat egg white-induced paw edema. The agar-well diffusion method was used to assess the *in vitro* antimicrobial activity of the test substances against a variety of microorganisms.

**Results:** The newly synthesized compounds HF7 and HF9, as shown in the molecular docking study findings with the cyclooxygenase-2 protein (PDB code: 4m11), exhibit binding energies of −9.247 and −8.716, respectively, which are greater than the reference docking result. During docking analysis using the *Saccharomyces cerevisiae* CYP51 receptor (PDB code: 4wmz), all synthesized compounds demonstrated higher docking scores compared to fluconazole, which served as the reference standard. The rat paw edema technique showed considerable action of HF6 and HF8 have a stronger impact compared to the standard impact. According to antimicrobial research results, HF8's (minimum inhibitory concentration [MIC]) against *Staphylococcus aureus* and *Streptococcus pyogenes* is 64 mcg/mL, whereas derivatives HF7 and HF11 also demonstrated MIC of 64 mcg/mL against *S. aureus*.

**Conclusion:** The effective synthesis of a new class of pyrazoline compounds was achieved. Most of the recently identified pyrazoline compounds were more effective against the microorganisms under investigation, with compounds HF7, HF8, and HF11 showing the greatest effectiveness in comparison to the standards used (fluconazole and amoxicillin).

**Keywords:** Molecular docking, Anti-inflammatory, Antimicrobial activity, Etodolac hydrazide, Pyrazoline.

 DOI: http://dx.doi.org/10.22159/ajpcr.2025v18i11.56550. Journal homepage: https://innovareacademics.in/journals/index.php/ajpcr

## INTRODUCTION

Medicinal chemistry includes the identification and creation of innovative medicinal compounds for disease management. This endeavor mostly concentrates on distinctive natural or synthetic organic compounds. Inorganic chemicals are important in therapy; nevertheless, organic molecules with specific pharmacological effects are clearly dominating [1].

The creative process of creating new drugs using biological target information is known as drug design. Drugs are usually small organic compounds that work by activating or inhibiting the action of biomolecules such as proteins. This allows the medicine to provide therapeutic benefits to the patient. In addition, drug design frequently employs computer modeling techniques, which are frequently referred to as "computer-aided drug design" [2].

Molecular docking represents a theoretical methodology in drug discovery, focusing on the prediction of the conformation, orientation, and binding affinity of receptor-ligand complexes. The concept of molecular docking, while straightforward, involves a complex process designed to assess energy scores across various models [3].

Nitrogen-containing heterocycles have garnered heightened interest for their possible application as medicinal agents in the treatment of numerous human ailments. Whether synthetic or naturally occurring, the nitrogen-containing indole structure is a component of many chemical frameworks that may perform a wide variety of biological activities in organic compounds. Etodolac, which is a non-steroidal anti-inflammatory drug (NSAID) and a member of the pyrano-carboxylic acid subgroup, is shown in Fig. 1. It is an NSAID medicine derived from indole-acetic acid. It provides analgesia and reduces inflammation to treat the disease rheumatoid arthritis. Similar to other NSAIDs, its principal mode of action is as an inhibitor of the cyclooxygenase (COX) [4].

Approved pharmacologically active NSAID derivatives were analyzed, leading to an examination of suitable structural modifications aimed at designing partial selective COX-2 inhibitors with enhanced activity [5]. Molecular changes of some classic NSAIDs enhanced their anti-inflammatory action relative to the parent drugs, often resulting in more inhibitory activity against COX-2 than COX-1. Molecular docking studies, employed as a prediction instrument, appear to corroborate the experimental findings [6].

In general, NSAIDs exhibit a broad spectrum of antimicrobial effects. They also significantly reduce adherence, biofilm formation, and other pathogenicity factors while influencing antibiotic susceptibility. Modifications in the structure of an NSAID enhance its antibacterial efficacy, and more research may provide effective antimicrobial agents [7].

By combining the etodolac structure with the heterocyclic moiety, it is possible to design a hybrid molecule that holds promise as an antimicrobial agent. This integration could enhance the compound's biological activity, paving the way for novel therapeutic applications. Shaik *et al.* demonstrated the successful synthesis and evaluation of a series of novel etodolac-based 1,2,4-triazole derivatives for their antibacterial properties. These compounds exhibited significant antibacterial activity against both Gram-positive Streptococcus pneumoniae and Gram-negative *Pseudomonas aeruginosa* [8].

In addition, Rabee and Tagreed (2025) focus on creating new NSAID derivatives using Gabapentin to affix an ester group to Etodolac, Ketorolac, and Tolmetin through an acetyl linker. The compounds that were produced (IIa-IVd) had high antibacterial activity and a strong anti-inflammatory impact; IVb was the least effective antimicrobial [9].

Heterocyclic compounds containing nitrogen atoms within their ring structures are of considerable importance in organic and medicinal chemistry, attributed to their varied structures and applications. Pyrazolines are a unique category of heterocyclic compounds that are distinguished by a five-membered saturated ring that contains two adjacent nitrogen atoms. Three of the positions are occupied by carbon and hydrogen atoms, with the endo-cyclic double bond located differently across the three pyrazoline isomers: 1-pyrazoline, 2-pyrazoline, and 3-pyrazoline. Among these, 2-pyrazoline emerges as the most stable configuration, as illustrated in Fig. 2 [10-12].

Pyrazolines and their derivatives are versatile compounds demonstrating a range of biological activities. Substituted pyrazolines and their derivatives demonstrate a variety of biological activities, including antimicrobial, anti-inflammatory, antidiabetic, analgesic, anti-lipoperoxidation, insecticidal, fungicidal, and herbicidal effects. Numerous derivatives of substituted pyrazolines exhibited significant anticancer activity against various tumors [13,14].

Chalcones serve as significant chemical building blocks in advanced chemistry, facilitating the synthesis of various compounds with biological activity. Their high reactivity is attributed to the α-β-unsaturated keto functional group, which is linked to numerous bioactivities, including anti-inflammatory, antimicrobial, antimalarial, antidiabetic, and anticancer properties [15].

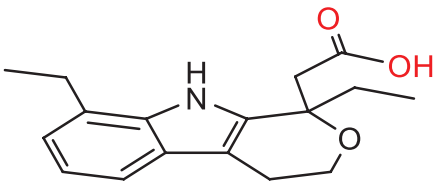


**Fig. 1: Etodolac chemical structure**

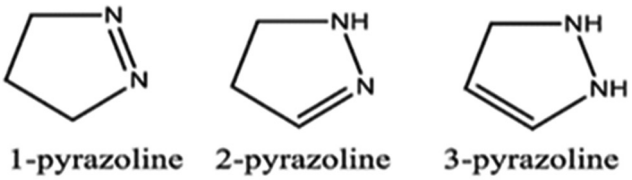


**Fig. 2: Isomers of pyrazoline**

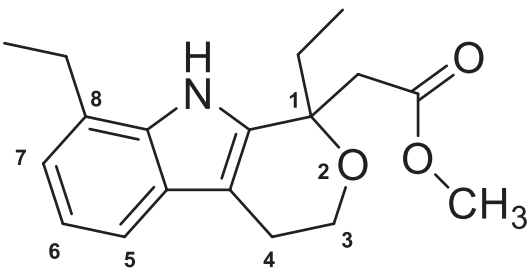


**Fig. 3: The produced etodolac methyl ester**

Our investigation centers on the production of innovative pyrazoline derivatives connected to etodolac, alongside the evaluation of their anti-inflammatory, antibacterial, and antifungal properties, drawing upon the previously documented biochemical and pharmacological characteristics of chalcone and pyrazoline.

## METHODS

### Molecular docking

Docking investigations were conducted using licensed Glide software integrated into version 13.0135 of Schrodinger's Maestro program. The first step was accessing the Protein Data Bank, followed by the docking procedure, which started with the retrieval of the crystalline structure of the COX-2 (PDB code: 4m11) using diclofenac as a reference [16], and the crystalline structure of the *Saccharomyces yeast* CYP51 receptor (PDB ID: 4wmz) using Fluconazole as a reference [17]. The LigPrep in the Maestro package was used to produce ligands using the force field OPLS_2005 after the ligand patterns were retrieved using the 2D Sketcher. The ligands were then produced in the lowest energy possible states at the target pH 7, desalted, and generated tautomers [18].

The extra-precision (XP) technique using Glide software, which is well-known for its exceptional accuracy in determining bound ligand configurations and affinities, was used to dock the produced ligands into the prepared proteins. For every ligand, docking simulations used the XP mode to generate and store three possible binding postures. Utilizing this technique, we assessed potential binding positions and predicted the binding patterns that would result in the highest energy stability between the ligand and the protein target [19].

### Absorption, distribution, metabolism, excretion (ADME) study

The study used Maestro–Schrodinger's QikProp tool to precisely forecast a variety of physicochemical and pharmacological characteristics. This program is renowned for its user-friendliness, accuracy, and rapidity in forecasting essential characteristics that elucidate the ADME and possible toxicity of drug-like molecules [20,21].

### Chemicals and instruments

The compounds used in this study were sourced from various commercial manufacturers, namely Sigma, Macklin, Thomas Baker, LOBA-Chemie, and HiMedia Ltd. TLC was used to track the reactions' development. Three solvent combinations were used in addition to the two solvent combinations in TLC. Stuart's (SMP3) melting point equipment was used to determine the melting point of compounds, and the results were uncorrected. The Fourier Transform Infrared spectrophotometer is produced by the Japanese company Shimadzu. A Bruker Ultra Shield spectrophotometer (400 and 500 MHz) was employed to obtain $^{1}$H-NMR spectra. The solvent employed for the testing of samples was dimethyl sulfoxide (DMSO)-d6, present at δ = 2.52 ppm.

### General procedure

The procedure for the production of all intermediate(s) and final compounds is detailed in Scheme 1. The interaction of acetophenone with different substituted aromatic aldehyde compounds yields chalcones I (a-f) as intermediates 1. In the second step, etodolac (carboxylic acid) is converted into etodolac methyl ester (compound A) in the presence of absolute methanol. Compound A then interacts with hydrazine hydrate to produce etodolac hydrazide (compound B), considered intermediate (2). With glacial acetic acid acting as a catalyst, intermediate(s) (1) and intermediate (2) combine to generate pyrazoline final products (HF6–11).

### Synthesis of chalcone intermediates (Ia-f)

Chalcone derivatives were synthesized by dissolving aromatic aldehydes (10 mmol) in 22 mL of 99% ethanol within a 250 mL round-

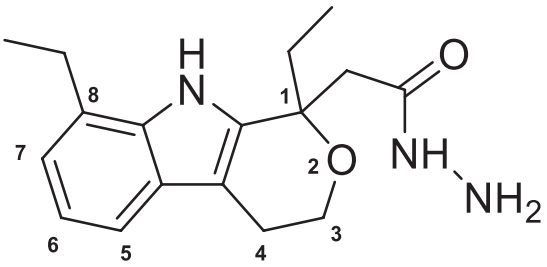

**Fig. 4: The produced etodolac hydrazide**

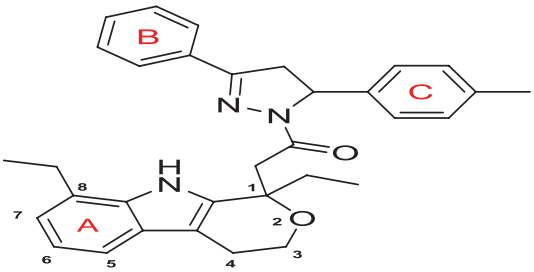

**Fig. 5: Final pyrazoline derivative (HF6)**

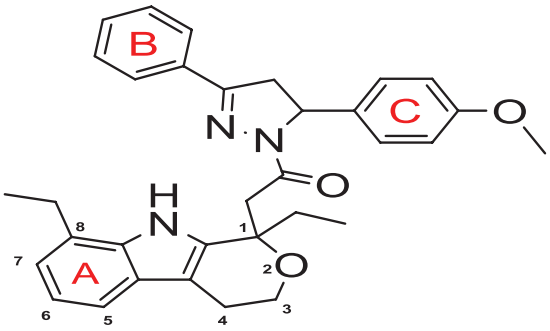

**Fig. 6: Final pyrazoline derivative (HF7)**

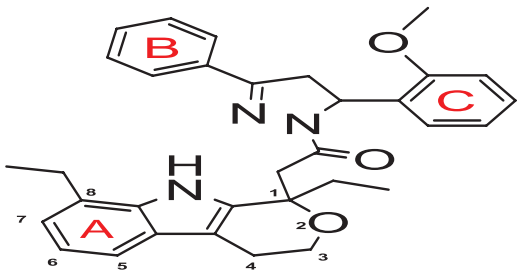

**Fig. 7: Final pyrazoline derivative (HF8)**

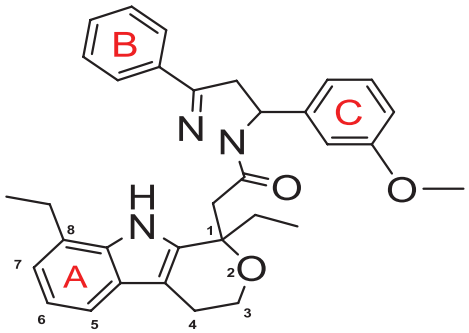

**Fig. 8: Final pyrazoline derivative (HF9).**

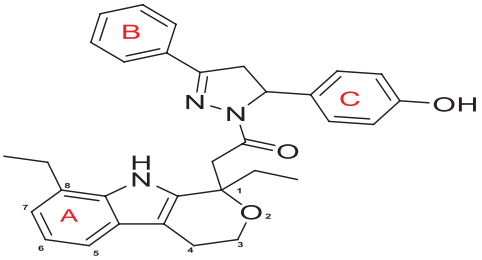

**Fig. 9: Final pyrazoline derivative (HF10)**

bottom flask, followed by the addition of acetophenone (1.17 mL, 10 mmol) Table 1. Ten milliliters of a 40% NaOH solution were gradually added over the course of 3 min while the reaction liquid remained cold in an ice bath. After that, the mixture was left to stir at 25°C for the whole night. Subsequently, the crude product underwent acidification with 2N HCl and was diluted with cold water. It was then filtered utilizing a Buchner funnel, and the solid product was further purified through recrystallization from ethanol [22,23].

**3-(4-methylphenyl)-1-phenyl-2-propen-1-one ($C_{16}H_{14}O$) (Ia)**
Deep yellow crystals, % of yield = 74%. M.P. = 96–97°C. ($R_f$: =0.56). ATR-FTIR ($\nu$ $cm^{-1}$): 3082 (CH stret. neighboring to the olefinic gr), 3055 (Asym. Stret. of aromatic CH), 2949 (Asym. Stret. of $CH_3$), 2860 (Sym. Stret. of $CH_3$), 1639 (C=O stret.), 1598, 1581, 1560 (stret. Vib. of aromatic and aliphatic C=C - overlapped).

**3-(4-methoxyphenyl)-1-phenylprop-2-en-1-one ($C_{16}H_{14}O_2$) (Ib)**
Light yellow powder, % of yield = 80%. M.P. = 74–75°C. ($R_f$: = 0.54). ATR-FTIR ($\nu$ $cm^{-1}$): 3059 (CH st. vib. neighboring to the olefinic gr.), 3059, 3016 (Asym. Stret. of aromatic CH), 2954, 2900 (Asym. Stret. of $CH_3$), 2843 (Sym. Stret. of $CH_3$), 1654 (C=O stret.), 1593, 1573, 1508 (stret. vib. C=C (aromatic and aliphatic overlap), 1261 (C-$OCH_3$stret. Vib.).

**3-(2-methoxyphenyl)-1-phenylprop-2-en-1-one ($C_{16}H_{14}O_2$) (Ic)**
Off-white powder, % of yield = 86 %. M.P. = 53–55°C. ($R_f$: = 0.80). ATR-FTIR ($\nu$ $cm^{-1}$): 3059, (CH st. vib. neighboring to the olefinic gr.), 3012 (Asym. Stret. of aromatic CH), 2956 (Asym. Stret. of $CH_3$), 2835 (Sym. Stret. of $CH_3$), 1658 (C=O stret.), 1597, 1546 (stret. vib. C=C (aromatic and aliphatic overlap), 1247 (C-$OCH_3$stret. Vib.).

**3-(3-methoxyphenyl)-1-phenylprop-2-en-1-one ($C_{16}H_{14}O_2$) (Id)**
Yellow crystals, % of yield = 75%. M.P.: 50–51°C, ($R_f$: =0.76). ATR-FTIR ($\nu$ $cm^{-1}$): 3074 (CH st. vib. neighboring to the olefinic gr.), 3007 (Asym. Stret. of aromatic CH), 2960, 2933 (Asym. Stret. of $CH_3$), 2831 (Sym. Stret. of $CH_3$), 1656 (C=O stret.), 1600, 1575 (stret. vib. C=C (aromatic and aliphatic overlap), 1265 (C-$OCH_3$stret. Vib.).

**3-(4-hydroxyphenyl)-1-phenylprop-2-en-1-one ($C_{15}H_{12}O_2$) (Ie)**
Bright yellow crystal, % of yield = 58%. M.P.: 181–183°C, ($R_f$: = 0.70). ATR-FTIR (v $cm^{-1}$): 3360-3080 Broad (Phenolic OH) stret., 3070 (CH st. vib. neighboring to the olefinic gr.), 3020 (Asym. Stret. of aromatic CH), 1647 (C=O stret.), 1597, 1577, 1554, 1508 (stret. vib. C=C (aromatic and aliphatic overlap), 1346 (OH bend. Vib.), 1215 (C-$OCH_3$stret. Vib.).

**3-(3-hydroxyphenyl)-1-phenylprop-2-en-1-one ($C_{15}H_{12}O_2$) (If)**
Off-white powder, % of yield = 70%. M.P.: 152–154°C, ($R_f$: = 0.45). ATR-FTIR (v $cm^{-1}$): 3331 Broad (Phenolic OH) stret., 3082 (CH st. vib. neighboring to the olefinic gr.), 3044 (Asym. Stret. of aromatic CH), 1651 (C=O stret.), 1593, 1570 Stret. vib. C=C (aromatic and aliphatic overlap), 1274 (OH bend. Vib.), 1217 (C-$OCH_3$stret. Vib.).

**Etodolac methyl ester synthesis [methyl 2-(1,8-diethyl-1,3,4,9-tetrahydropyrano [3,4-b] indol-1-yl) acetate] (compound A) Fig. 3:**
A clear solution was prepared in a 250 mL round-bottomed flask by thoroughly mixing methanol (25 mL) with etodolac powder (0.021 mol,

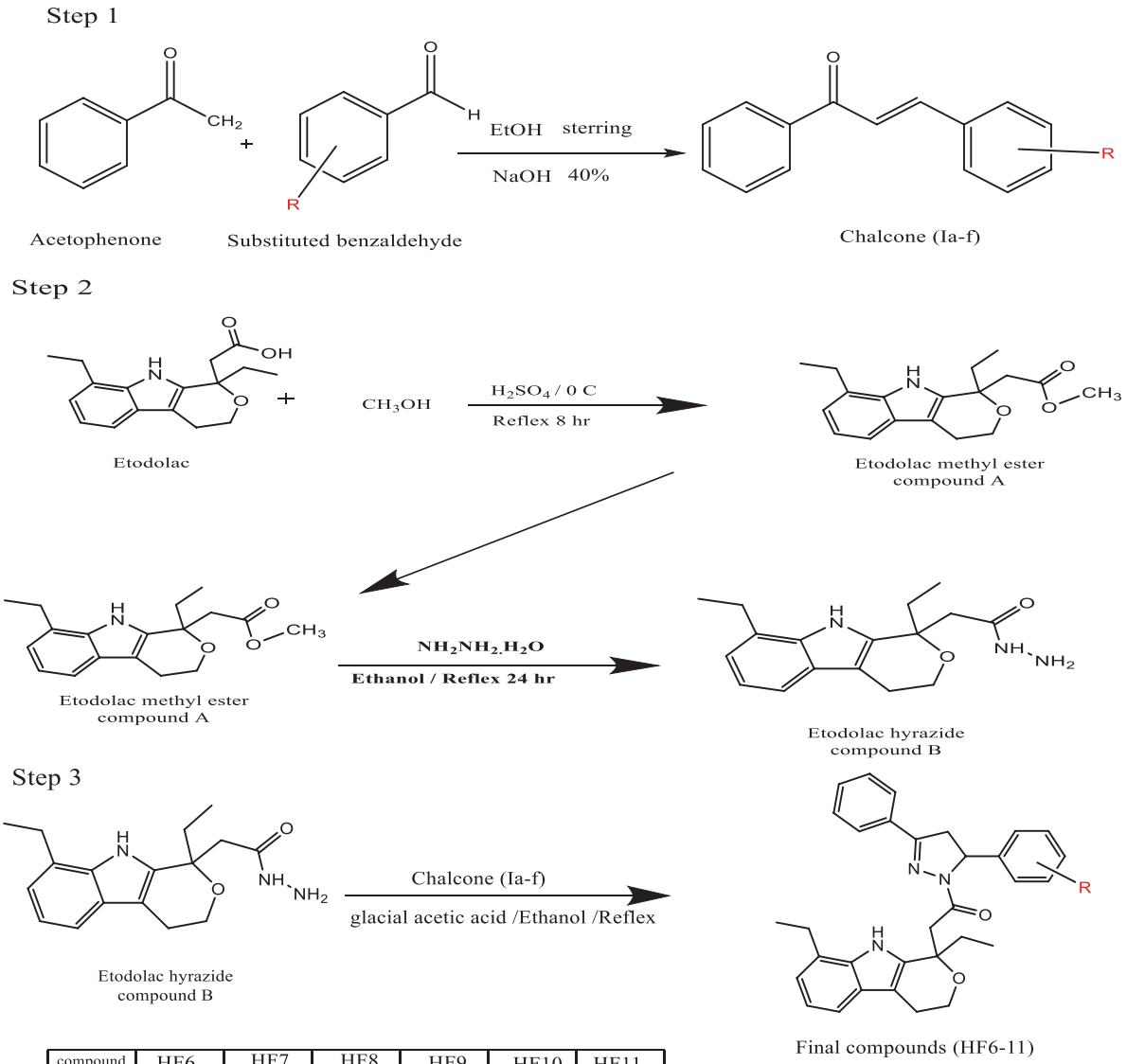


| compound | HF6 | HF7 | HF8 | HF9 | HF10 | HF11 |
|---|---|---|---|---|---|---|
| R group | p -$CH_3$ | p -$OCH_3$ | o -$OCH_3$ | m -$OCH_3$ | p -OH | m -OH |

**Scheme 1. The sequential chemical synthesis process for both the intermediate products and the final compounds**

6 g). After cooling in an ice bath to 0°C, add to the solution gradually 0.5 mL of concentrated $H_2SO_4$ while stirring continuously. The reaction mixture underwent continuous reflux for 8 h, accompanied by magnetic stirring to ensure proper mixing. The reaction's progress was tracked using TLC, employing a solvent system consisting of a 1:1 ratio of ethyl acetate and petroleum ether (boiling range 60–80°C). Once the mixture had cooled to room temperature, 40 mL of chilled DW was introduced. A fully saturated solution of bicarbonates of sodium (5% w/v) was carefully added to neutralize any residual acid. This process led to the precipitation of etodolac methyl ester in the form of a pale yellow powder [24]. During filtering, the precipitate was collected, allowed to dry completely, and then washed with cold distilled water. After that, 100% ethanol was used to recrystallize it. % of the yield = 76%, m.p. (126–128°C). $R_f$ = 0.74. ATR-FTIR ($\nu$ $cm^{-1}$): 3379: (N-H, indole stretching), 3062, 3030: aromatic (C-H) stretching, 2978: asymm. Stretching (C-H) of aliphatic ($CH_3$ and $CH_2$), 2873: symm. Stretching (C-H) of aliphatic ($CH_3$ and $CH_2$), 1708: (C=O) Stretching of (ester) band, 1234: (C-O-C) Stretching.

**Synthesis method of N'-[2-(1,8-diethyl-1,3,4,9-tetrahydropyrano[3,4-b]indol-1-yl)-acetyl]-hydrazine (etodolac hydrazide) (B compound) Fig. 4:**

A solution of compound (A) (0.01 moles, 3 g) dissolved in 50 mL of 100% ethanol was added to a leftover quantity of hydrazine hydrate (99%) (0.2 moles, 10 mL) in a 150 mL round-bottom flask. At 80°C, the mixture was refluxed until a single spot was seen in TLC using a solvent system consisting of hexane, ethyl acetate, and methanol (5.5:3:1.5), which indicates that the reaction has been completed. After the reflux process was completed, the mixture was left to cool to approximately 25°C. Once it reached this temperature, cold distilled water was introduced into the reaction flask, triggering the formation of a white precipitate. The precipitate was then left undisturbed overnight [25]. Filtration was applied to the resulting white precipitate, followed by several rinses with cold distilled water, drying, and finally, recrystallization using hot ethanol. Yield = 64%, m.p.:188–190°C. $R_f$ value = 0.46. ATR-FTIR ($\nu$ $cm^{-1}$): 3365, 3315: (N-H) of (Indole and hydrazide stretching), 3062: (C-H) stretching aromatic, 2966, 2910: asymm. Stretching (C-H) of aliphatic ($CH_3$ and $CH_2$), 2871: symm. stretching (C-H) of aliphatic ($CH_3$ and $CH_2$), 1651: (C=O) (amide str.), 1620: (N-H) bend., 1238: (C-O-C) str.

**New pyrazoline derivatives synthesis (final compounds) (HF6-HF11)**

The compounds (HF6-HF11) were synthesized by mixing and dissolving a combination of compound B (1 mmole) and one chalcone derivative (1a-f) (1 mmole) in 20 mL of ethanol. After 15 min, reflux was applied to the mixture. A catalytic amount of glacial acetic acid was added, and the mixture was allowed to reflux for approximately 24 h. The reaction

time was evaluated using thin-layer chromatography in order to get an individual spot [26]. After cooling, the reaction mixture is added to 20 mL of cold water to trigger the result to precipitate. The product has undergone two cold water washes, filtration, and drying. The re-crystallized procedure was then carried out using heated ethanol.

*2-(1,8-diethyl-1,3,4,9-tetrahydropyrano[3,4-b]indol-1-yl)-1-(3-phenyl-5-(p-tolyl)-4,5-dihydro-1H-pyrazol-1-yl)ethan-1-one (HF6) Fig. 5:*

Brown powder, yield = 60%, M.P. = (146–148)°C, $R_f$= 0.64. ATR-FTIR ($\nu$ $cm^{-1}$): 2294: Indole (NH) str., 3053: arom. (C-H) str., 2962, 2929: (C-H asymm. str.) of ($CH_3$ and $CH_2$), 2873: (C-H symm. str.) of ($CH_3$ and $CH_2$), 1660: (C=O) str. band, 1597: (str. of C=N), 1556: arom (C=C) str., 1215: (C-O-C) str.

$^1$HNMR (δ ppm): 0.63 (t, 3H, -$CH_3$ at C1 dihydro-pyran ring), 1.27 (t, 1H, -$CH_3$ at C8 ring A), 2.04 (q, 2H, (-$CH_2$- at C1 dihydro-pyran ring), 2.14 (q, 2H, -$CH_2$- at C8 ring A), 2.22 (s, 3H, -$CH_3$ attached at ring C), 2.6, 2.66 (2dd, 2H, -$CH_2$- ∝ to (C=O)), 2.78 (m, 2H, C4 dihydro-pyran ring), 2.89 (m, 2H, C3 dihydro-pyran ring), 3.84, 3.91, 5.53 (3dd, 3H, pyrazoline ring protons), 6.86, 6.90 (2d, 2H, ring A-Ar. protons), 7.13 (d, 2H, ring C- Ar. protons), 7.18 (t, 1H, ring A-Ar. proton), 7.24 (d, 2H, ring C-Ar. protons), 7.31–7.73 (m, 3H, ring B-Ar. protons), 7.9 (d, 2H, ring B-Ar. protons), 10.58 (s, 1H, N-H Indole).

*2-(1,8-diethyl-1,3,4,9-tetrahydropyrano[3,4-b]indol-1-yl)-1-(5-(4-methoxyphenyl)-3-phenyl-4,5-dihydro-1H-pyrazol-1-yl)ethan-1-one (HF7) Fig. 6:*

Deep yellow crystal, yield = 68%, M.P. = (132–134)°C, $R_f$= 0.58. ATR-FTIR ($\nu$ $cm^{-1}$): 3309: Indole (NH) str., 3055: arom. (C-H) str., 2962, 2931: (C-H asymm. str.) of ($CH_3$ and $CH_2$), 2839: (C-H symm. str.) of ($CH_3$ and $CH_2$), 1643: (C=O) str. band, 1597: (str. of C=N), 1573, 1512: arom. (C=C) str., 1247: (C-O-C) str.

$^1$HNMR (δ ppm): 0.63 (t, 3H, -$CH_3$ at C1 dihydro-pyran ring), 1.23 (t, 1H, -$CH_3$ at C8 ring A), 2.07 (q, 2H, [-$CH_2$- at C1 dihydro-pyran ring]), 2.14 (q, 2H, [-$CH_2$- at C8 ring A]), 2.6, 2.66 (2dd, 2H, -$CH_2$- ∝ to (C=O)), 2.81 (m, 2H, C4 dihydro-pyran ring), 2.87 (m, 2H, C3 dihydro-pyran ring), 3.84(s, 3H, O-$CH_3$ attached at ring C), 3.91, 4.01, 5.56 (3dd, 3H, pyrazoline ring protons), 6.88 (d, 2H, ring C- Ar. protons), 6.95, 7.01 (2d, 2H, ring A-Ar. protons), 7.13 (t, 1H, ring A-Ar. proton), 7.24 (d, 2H, ring C-Ar. protons), 7.32–7.82 (m, 3H, ring B-Ar. protons), 7.88 (d, 2H, ring B-Ar. protons), 10.47 (s, 1H, N-H Indole).

*2-(1,8-diethyl-1,3,4,9-tetrahydropyrano[3,4-b]indol-1-yl)-1-(5-(2-methoxyphenyl)-3-phenyl-4,5-dihydro-1H-pyrazol-1yl)ethan-1-one Fig. 7:*

light beige powder, yield = 65%, M.P. = (118–121)°C, $R_f$= 0.66. ATR-FTIR ($\nu$ $cm^{-1}$): 3298: Indole (NH) str., 3051: arom. (C-H) str., 2960, 2929: (C-H asymm. str.) of ($CH_3$ and $CH_2$), 2872: (C-H symm. str.) of ($CH_3$ and $CH_2$), 1662: (C=O) str. band, 1597: (str. of C=N), 1570: arom. (C=C) str., 1246: (C-O-C) str.

$^1$HNMR (δ ppm): 0.65 (t, 3H, -CH3 at C1 dihydro-pyran ring), 1.28 (t, 1H, -CH3 at C8 ring A), 2.04 (q, 2H, -CH2- at C1 dihydro-pyran ring), 2.13 (q, 2H, -CH2- at C8 ring A), 2.63, 2.71 (2dd, 2H, -CH2- ∝ to (C=O)), 2.83 (m, 2H, C4 dihydro-pyran ring), 2.89 (m, 2H, C3 dihydro-pyran ring), 3.84 (s, 3H, O-$CH_3$ attached at ring C), 3.92, 4.00, 5.53 (3dd, 3H, pyrazoline ring protons), 6.91 (d, 1H, ring C- Ar. protons), 6.96, 7.05 (2t, 2H, ring C-Ar. protons), 7.10, 7.12 (2d, 2H, ring A- Ar. proton), 7.20 (t, 1H, ring A-Ar. protons), 7.27 (d, 1H, ring C-Ar. protons), 7.32–7.79 (m, 3H, ring B-Ar. protons), 7.90 (d, 2H, ring B-Ar. protons), 10.56 (s, 1H, N-H Indole).

*2-(1,8-diethyl-1,3,4,9-tetrahydropyrano[3,4-b]indol-1-yl)-1-(5-(3-methoxyphenyl)-3-phenyl-4,5-dihydro-1H-pyrazol-1-yl)ethan-1-one Fig. 8:*

Light brown crystal, yield = 60%, M.P. = (126–128)°C, $R_f$= 0.68. ATR-FTIR ($\nu$ $cm^{-1}$): 3304: Indole (NH) str., 3053: arom. (C-H) str., 2960, 2929: (C-H asymm. str.) of ($CH_3$ and $CH_2$), 2872: (C-H symm. str.) of ($CH_3$ and $CH_2$), 1653: (C=O) str. band, 1602: (str. of C=N), 1579, 1508: arom. (C=C) str.,1257: (C-O-C) str.

$^1$HNMR (δ ppm): 0.63 (t, 3H, -CH3 at C1 dihydro-pyran ring), 1.27 (t, 1H, -CH3 at C8 ring A), 1.98 (q, 2H, -CH2- at C1 dihydro-pyran ring), 2.04 (q, 2H, -CH2- at C8 ring A), 2.62, 2.69 (2dd, 2H, -CH2- ∝ to (C=O)), 2.82 (m, 2H, C4 dihydro-pyran ring), 3.01 (m, 2H, C3 dihydro-pyran ring), 3.68 (s, 3H, O-CH3 attached at ring C), 3.80, 3.97, 5.56 (3dd, 3H, pyrazoline ring protons), 6.90 (d, 1H, ring C- Ar. protons), 6.96 (s, 1H, ring C- Ar. protons), 7.03 (d, 1H, ring C-Ar. protons), 7.06, 7.09 (2d, 2H, ring A- Ar. proton), 7.21 (t, 1H, ring A-Ar. protons), 7.26 (t, 1H, ring C- Ar. protons), 7.33–7.78 (m, 3H, ring B-Ar. protons), 7.95 (d, 2H, ring B-Ar. protons), 10.59 (s, 1H, N-H Indole).

*2-(1,8-diethyl-1,3,4,9-tetrahydropyrano[3,4-b]indol-1-yl)-1-(5-(4-hydroxyphenyl)-3-phenyl-4,5-dihydro-1H-pyrazol-1-yl)ethan-1-one Fig. 9:*

Yellow powder, yield = 58%, M.P. = (190–193)°C, $R_f$= 0.47. ATR-FTIR ($\nu$ $cm^{-1}$): 3302-3110 broad: (NH) str. of indole overlapped with OH stretching band, 3066, 3020: arom. (C-H) str., 2966, 2931: (C-H asymm. str.) of ($CH_3$ and $CH_2$), 2860: (C-H symm. str.) of ($CH_3$ and $CH_2$), 1651: (C=O) str. band, 1600: (str. of C=N), 1581, 1558, 1508: arom. (C=C) str., 1215: (C-O-C) str.

$^1$HNMR (δ ppm): 0.63 (t, 3H, -$CH_3$ at C1dihydro-pyran ring), 1.27 (t, 1H, -$CH_3$ at C8 ring A), 2.02 (q, 2H, (-$CH_2$- at C1 dihydro-pyran ring), 2.08 (q, 2H, (-$CH_2$- at C8 ring A), 2.60, 2.66 (2dd, 2H, -$CH_2$- ∝ to (C=O)), 2.74 (m, 2H, C4 dihydro-pyran ring), 2.84 (m, 2H, C3 dihydro-pyran ring), 3.94, 4.00, 5.52 (3dd, 3H, pyrazoline ring protons), 6.72,6.87 (2d, 4H, ring C- Ar. protons), 6.9, 6.94 (2d, 2H, ring A-Ar. protons), 7.25 (t, 1H, ring A- Ar. proton), 7.54-7.72 (m, 3H, ring B-Ar. protons), 7.78 (d, 2H, ring B-Ar. protons), 8.99 (s, 1H, -OH proton), 10.60 (s, 1H, N-H Indole).

*2-(1,8-diethyl-1,3,4,9-tetrahydropyrano[3,4-b]indol-1-yl)-1-(5-(3-hydroxyphenyl)-3-phenyl-4,5-dihydro-1H-pyrazol-1-yl)ethan-1-one Fig. 10:*

Brown powder, yield = 66%, M.P. = (174–176)°C, $R_f$= 0.66. ATR-FTIR ($\nu$ $cm^{-1}$): 3470-3210 broad: OH stretching overlapped with (NH) str. of indole, 3067: arom. (C-H) str., 2962: (C-H asymm. str.) of ($CH_3$ and $CH_2$), 2927: (C-H symm. str.) of ($CH_3$ and $CH_2$), 1661: (C=O) str. band, 1614: (str. of C=N), 1543, 1527: arom. (C=C) str., 1215: (C-O-C) str.

$^1$HNMR (δ ppm): 0.64 (t, 3H, -$CH_3$ at C1dihydro-pyran ring), 1.25 (t, 1H, -$CH_3$ at C8ring A), 2.01 (q, 2H, (-$CH_2$- at C1dihydro-pyran ring), 2.11 (q, 2H, (-$CH_2$- at C8ring A), 2.63, 2.74 (2dd, 2H, -$CH_2$- ∝ to (C=O)), 2.84 (m, 2H, C4 dihydro-pyran ring), 2.92 (m, 2H, C3 dihydro-pyran ring), 3.88, 4.02, 5.54 (3dd, 3H, pyrazoline ring protons), 6.82 (s, 1H, ring C- Ar. protons), 6.88 (d, 2H, ring C- Ar. protons), 6.94, 6.99 (2d, 2H, ring A-Ar. protons), 7.13 (t, 1H, ring C- Ar. protons), 7.23 (t, 1H, ring A- Ar. proton), 7.51–7.72 (m, 3H, ring B-Ar. protons), 7.84 (d, 2H, ring B-Ar. protons), 9.02 (s, 1H, -OH proton), 10.58 (s, 1H, N-H Indole).

**Initial pharmacological investigation**

*Anti-inflammatory activity*

This study's foundation is the evaluation of (HF6–11) synthetic chemicals' anti-inflammatory efficacy using the paw edema technique, using egg albumin-induced rat paw edema in contrast to traditional drugs.

*Techniques*

The main indicator of the produced compound's efficacy in an *in vivo* anti-inflammatory investigation with albino rats was its capacity to lessen the thickness of the rodents' paw edema. After being acquired from Baghdad University's Animal House, 48 albino rats weighing 150–200 g were kept at the Iraqi Center for Cancer and Medical-Genetics Research. During their acclimation period, the rodents were maintained in standard conditions with unlimited access to water and fed a diet of

commercial chow. Egg whites were subcutaneously injected into the rat paw to assess inflammation at both the onset and throughout the short-term experiment. The study included seven distinct groups of animals, with each group consisting of six rats.

Group A consisted of six rodents designated as the control group, receiving a 50% v/v solution of propylene glycol as the administered vehicle.

In Group B, six animals received a dosage of diclofenac sodium (3 mg/kg) diluted in 50% propylene glycol.

Groups H, I, J, K, L, and M, each consisting of seven rodents, received injections containing prepared compounds diluted in propylene glycol and measured, as detailed in Table 2.

A 0.05 mL subcutaneous application of undiluted egg-white substance may cause significant inflammation, particularly in the hind paws, and consequent skin irritation in the plantar region of the rat's left hind leg. Paw width was assessed using a Vernier caliper at specific time intervals—0, 30, 60, 120, 180, 240, and 300 min—after administering either the target compounds or the vehicle, with measurements beginning 30 min post-injection [27,28].

*Determining the dose*

The suggested dosages of these targeted drugs were determined using the following formula:[28]

$$\frac{Dose\ of\ reference\ compound}{M.wt\ of\ reference\ compound} = \frac{Dose\ of\ tested\ compound}{M.wt\ of\ tested\ compound}$$

The desired compounds are found using an equation, as shown in Table 2.

*In vitro antimicrobial test*

The synthesized derivatives (HF6–11) were evaluated for their antimicrobial properties toward various microorganisms, which included Gram (+)-positive bacterial strains such as *Streptococcus pyogenes* and *Staphylococcus aureus*, Gram (-)-negative bacteria such as *P. aeruginosa* and *Escherichia coli*, as well as fungi such as *Candida albicans*. The agar-diffusion technique, the minimum inhibitory concentration (MIC), and minimum bactericidal concentration (MBC) were all determined at Iraq's Cac-Center for Research and Testing, and were used in the assessment. For bacterial purposes, we used amoxicillin and ciprofloxacin, and for fungal purposes, we used fluconazole. As a solvent, DMSO was used for the negative control. In the study on antibacterial agents, the bacterial strains that were utilized were resistant strains, with *S. aureus* and *E. coli* being the most resistant types.

*Part for statistical analysis*

All experiments were conducted and reported in triplicate. Mean values were presented alongside standard deviation (SD) figures. Before analysis, data were evaluated for normality and homogeneity. The Kruskal–Wallis test and One-Way ANOVA were then applied to compare the means and assess statistical significance, with thresholds set as significant (<0.05), highly significant (**<0.01), and very highly significant (***<0.001). Statistical analyses were performed using SPSS Version 23, whereas correlations and visualizations were generated with Origin-Lab 2021 software.

## RESULTS AND DISCUSSION

### Chemistry

The synthesis of chalcone intermediate(s) (Ia-f) was accomplished by the use of the aldol condensation technique. An aqueous solution of sodium hydroxide in 40% ethanol was used to react substituted aromatic aldehydes with acetophenone in this procedure. Chalcones were subjected to FTIR analysis, which confirmed the existence of C=O stretching at the 1662–1647 spectral range.

**Table 1: Aromatic aldehydes and their weights**

| Aldehydes' name | Compound symbol | R-group | Weight (g) |
|---|---|---|---|
| 4-Methyl-benzaldehyde | Ia | p-$CH_3$ | 1.2 |
| 4-Methoxy-benzaldehyde | Ib | p-$OCH_3$ | 1.36 |
| 2-Methoxy-benzaldehyde | Ic | o-OCH3 | 1.36 |
| 3-Methoxy-benzaldehyde | Id | m-OCH3 | 1.36 |
| 4-Hydroxy-benzaldehyde | Ie | p-OH | 1.22 |
| 3-Hydroxy-benzaldehyde | If | m-OH | 1.22 |

**Table 2: The (HF6–11) derivatives, and diclofenac molecular weights and dosages**

| Compound | M.wt (g/mol) | Dose (mg/kg) |
|---|---|---|
| Diclofenac sodium | 318.1 | 3 |
| HF6 | 505.658 | 4.768 |
| HF7 | 521.658 | 4.919 |
| HF8 | 521.658 | 4.919 |
| HF9 | 521.658 | 4.919 |
| HF10 | 507.631 | 4.787 |
| HF11 | 507.631 | 4.787 |

After reacting etodolac (raw powder) in methanol with a few milliliters of concentrated hydrosulfuric acid as a catalyst, the methyl ester of etodolac, which is referred to as Compound (A), was formed. By combining etodolac methyl ester with hydrazine hydrate (NH2NH2. H2O), the chemical (B) was produced as a result of the reaction. The synthesis of the new pyrazoline derivatives involves the reaction of etodolac hydrazide with a range of chalcones (Ia-f), utilizing glacial acetic acid as the catalyst for the reaction.

### Docking study

The docking results for the final derivatives (HF6–11) were analyzed, focusing on their binding modes, positions, and binding energies. In this study, we attempted to deduce how the COX-2 protein (PDB code: 4m11) and the CYP51 receptor (PDB code: 4wmz) in *Saccharomyces cerevisiae* interact with the ligands that were created. Results from the docking study show that the ligand interacts with the protein according to the preferred method's stringent protocol. The final pyrazoline derivatives, with the exception of the HF10 derivative, displayed a stronger affinity for COX-2 compared to the docking score results of both the reference ligand (diclofenac) and the parent compound (etodolac), as illustrated in Table 3. Furthermore, all final pyrazoline derivatives exhibited a greater affinity for the *S. cerevisiae* CYP51 receptor than the docking score result of the reference ligand, fluconazole, as shown in Table 4.

The analysis of the docking results shows that modifying the position of the substituted group (R group) significantly impacts the docking score. For instance, comparing the docking scores of HF10 and HF11 demonstrates an almost twofold increase in the score. The (2D) and (3D) interactions are illustrated in Figs. 11 and 13.

Two protein targets were measured for root mean square deviation (RMSD) by comparing the docked ligand configuration to its original co-crystallized one. Protein structures with a degree of RMSD <1 Å have excellent agreement, which is frequently observed in high-resolution structures. 1–2 Å: Good agreement, usually suitable for the majority of research. 2–3 Å: Moderate agreement; depending on the situation, it could be appropriate. 3 Å: Poor agreement, which frequently denotes notable variations. The RMSD values were below 2 Å for both proteins, suggesting a stable interaction between the ligand and protein and a successful docking process, as shown in Figs. (12 and 14) [29].

The interaction revealed that the synthesized compounds achieved notable results by forming one or two hydrogen bonds with the residues ARG120 and TYR355, in addition to establishing a Pi-cation bond with ARG120. Both types of bonds play a crucial role in catalysis and binding.

**Table 3: Anti-inflammatory docking values with COX-2 (PDB Code: 4m11)**

| ID ligand | ΔG (Kcal/mol) | Interaction types |
|---|---|---|
| Diclofenac (standard) | −7.389 | Halogen bonding occurs with SER530, whereas two hydrogen bonds are formed with ARG120 and TYR355. In addition, a pi-cation interaction is observed with ARG120. |
| Etodolac (parent) | −7.335 | Hydrogen bonding interactions involving ARG120 and π-cation interactions with ARG120. |
| HF6 | −8.244 | Hydrogen bonds formed with ARG120 and TYR355. |
| HF7* | −9.247 | Two hydrogen bonds are formed with ARG120, and one hydrogen bond is established with TYR355. |
| HF8 | −8.201 | Two hydrogen bonds are formed with ARG120 and TYR355, whereas ARG120 also engages in a pi-cation interaction. |
| HF9* | −8.716 | Two hydrogen bonds with ARG120 and one hydrogen bond with TYR355. |
| HF10 | −5.793 | Hydrogen bonding involves the proton of indole with VAL116, alongside a pi-cation interaction with ARG120. |
| HF11 | −8.078 | Two hydrogen bonds are formed with ARG120 and TYR355. |

*Final synthesized compounds: HF7, and HF9 give high docking score.

**Table 4: Antifungal docking scores: (PDB code 4wmz)**

| ID | ΔG (Kcal/mol) | Interaction types |
|---|---|---|
| Fluconazole (standard) | −6.479 | 2H-Bonds with (TYR 140, CYS 470) |
| HF6* | −10.725 | H-Bond with (CYS 470) |
| HF7 | −8.700 | Hydrophobic and polar interactions |
| HF8 | −9.166 | H-Bonds with (TYR 140) |
| HF9* | −10.807 | H-Bond with (CYS 470), Pi-cation with (LYS 151) |
| HF10 | −9.871 | H-Bonds with (GLN 150, ILE 471), Pi-cation with (LYS 151) |
| HF11* | −10.540 | 2H-Bonds with (TYR 140, PRO 462) |

*Final synthesized compounds: HF6, HF9, and HF11 give high docking score.

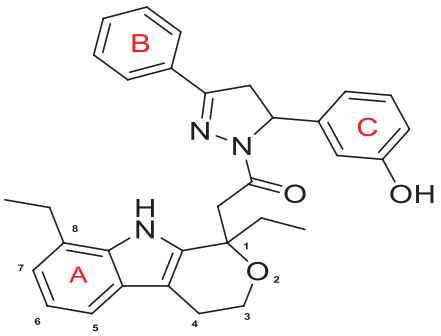


**Fig. 10: Synthesized pyrazoline (HF11)**

**Structure-activity relationship (SAR)**

The pharmacological behavior of pyrazoline derivatives is heavily influenced by the specific groups linked to various positions within the pyrazoline core. Consequently, both steric hindrance and electronegative properties at the N-1, C-3, and C-5 positions play a critical role in shaping their pharmacokinetic profiles [30].

Derivatives of the starting structure with functional groups such as OCH3 increase their potential to act as inhibitors of biological targets. The type position of the substituted group is very important for activity; it is clear that HF7 *(*p-methoxy) gives a higher score for COX-2 than HF9 (*m*-methoxy), although the two compounds give the same interaction bond with amino acids of the target protein, but the steric factor decreases the force of hydrogen bonding [31].

With the same target 4m11, HF10 (*p*-hydroxy) gives the worst score (−5.793) among the other compounds, and <HF11 (*o*-hydroxy), which gives a docking score (−8.078).

Despite having a wide range of pharmacological properties, little is known about the toxicity and therapeutic consequences of pyrazoline derivatives. As of right now, research on SARs and the hybridization of their molecules suggests safer, more transparent treatments [30].

**ADME studies**

Any pharmaceutical product development or improvement must begin with an assessment of the ADME characteristics of drug-like substances. The characteristics of the final compounds (HF6–11) were forecasted through *in silico* methods using a range of pharmacokinetic parameter values. Table 5 presents the virtual assessment of drug-like molecular properties, utilizing the rule of five, the rule of three, oral absorption parameters, and an analysis of central nervous system (CNS) penetration. Each of the produced compounds clearly follows the three-value rule and the five principles of Lipinski that fall inside the domain of two. On the other hand, they exhibit outstanding oral absorption in humans.

The metabolic liability of the investigated compounds is considered moderate. Computational predictions indicate that compounds such as HF2, HF3, and HF4 are likely to undergo substantial metabolic biotransformation. These findings warrant experimental validation through *in vitro* microsomal stability assays.

The topological polar surface area (TPSA) values for all compounds were within the optimal range (≤90 $Å^2$), with HF1, HF2, HF3, and HF6 displaying particularly favorable TPSA values (~45 $Å^2$). Such low scores are advantageous for both intestinal absorption and blood–brain barrier (BBB) permeation. Predicted CNS activity scores ranged between −1 and 1. Compounds HF1, HF2, HF3, and HF6 exhibited positive CNS activity scores, indicating their potential to cross into the CNS, a desirable property for CNS-focused therapeutic agents.

**Research on anti-inflammatory**

Table 6 presents the statistical analysis of the anti-inflammatory activity of six tested compounds (HF6, HF7, HF8, HF9, HF10, and HF11), compared with a control and a standard drug, over a time course from 0 to 5 h. The normality of the data at each time point was evaluated using the Shapiro–Wilk test. With the exception of the 1/2-h time point, the results indicated that the data were not normally distributed ($p>0.05$), prompting the use of the non-parametric Kruskal–Wallis test. For the 1/2-h data, which passed the normality test, one-way ANOVA was applied.

These findings are consistent with recent studies. For instance, Orján *et al.* [32] demonstrated that bioactive compounds derived from medicinal plants exhibit significant time-dependent anti-inflammatory effects when analyzed with appropriate non-parametric methods, such as the Kruskal–Wallis test, particularly when data do not conform to normality.

Figs. (15 and 16), the histogram showing the levels of six compounds (HF6, HF7, HF8, HF9, HF10, and HF11) along with control and standard groups, measured over time from 0 to 5 h. As illustrated, all

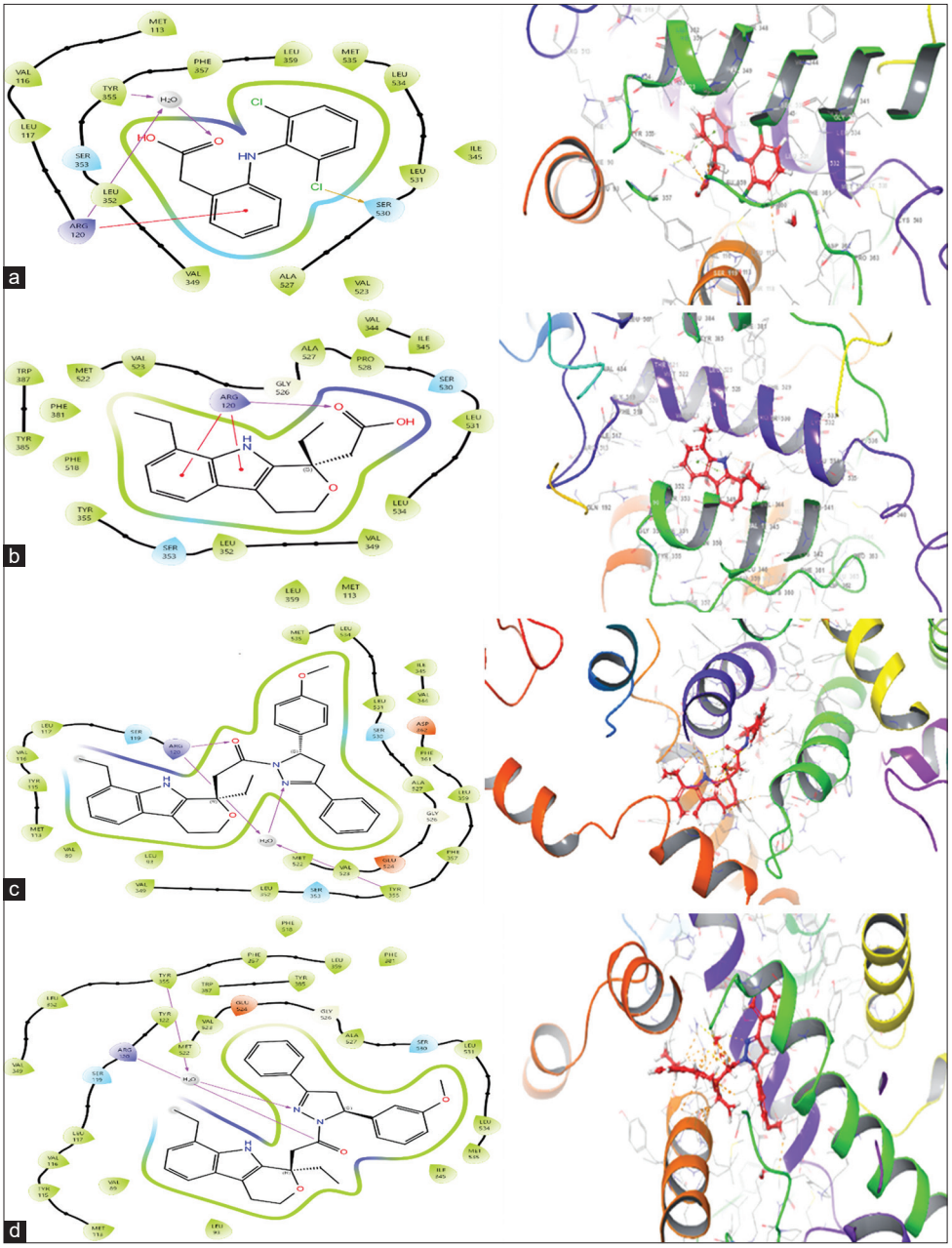


**Fig. 11: Standard, Parent, and Highest Score Docked Ligands with 4M11 Protein. (a) Diclofenac (Standard), (b) Etodolac (raw compound), (c) Derivative HF7, (d) Derivative HF9**

**Table 5: Results from the manufactured compounds' *in-silico* absorption, distribution, metabolism, and excretion testing**

| Compounds | Mol. wt | Donor HB | Accept HB | #Metab | Percent oral absorption | CNS | Topological polar surface area Å2 | Rule of five | Rule of three |
|---|---|---|---|---|---|---|---|---|---|
| HF6 | 505.658 | 1 | 4 | 7 | 100 | 1 | 45.535 | 2 | 2 |
| HF7 | 521.658 | 1 | 5 | 7 | 100 | 0 | 58.373 | 2 | 2 |
| HF8 | 521.658 | 1 | 5 | 8 | 100 | 0 | 49.548 | 2 | 2 |
| HF9 | 521.658 | 1 | 5 | 8 | 100 | 0 | 61.683 | 2 | 2 |
| HF10 | 507.631 | 2 | 5 | 7 | 100 | 0 | 68.194 | 2 | 2 |
| HF11 | 507.631 | 2 | 5 | 8 | 100 | 0 | 75.869 | 2 | 2 |
| Recommended values | 130–725 | 0–6 | 2–20 | 1–8 | >80% is high <25% is poor | −2(less activity)−2 (more activity) | 20–130 Å2 | Max 4 | Max 3 |

M.Wt: The molecular weight of the ligand, HBD: Is the estimated amount of hydrogen bonds that a solute in a water solution will provide to water molecules. HBA: Is the estimated amount of hydrogen bonds that a solute in a water solution may accept from water molecules, %Human oral absorption: As a percentage, oral absorption in humans is measured as %, CNS: Predicted activity of the CNS on a scale from−2 (inactive) to+2 (active), TPSA: Stands for topological polar surface area; Å$^2$, Rule of five: Tally of violations of Lipinski's five-limit restriction, Here are the criteria: mol_M.Wt must be <500, QPlog (Po/w) must be <5, donor-HB must be ≤5, and accpt-HB must be ≤10. To be considered drug-like, a compound must fulfill these requirements, including the following elements: a QPlogS value more than−5.7, a QP PCaco value higher than 22 nm/s, and #metab <7 CNS: Central nervous system

**Table 6: This study compared the anti-inflammatory effects of six different compounds across a range of time points, from 0 to 5 h, using different groups: control, standard, HF6, HF7, HF8, HF9, HF10, and HF11**

| Paw thickness (mm±SD) | | | | | | | |
|---|---|---|---|---|---|---|---|
| **Time (h)** | **0 h** | **0.5 h** | **1 h** | **2 h** | **3 h** | **4 h** | **5 h** |
| Control | 4.43±0.03 | 4.66±0.02 | 6.00±0.03 | 7.61±0.5 | 7.7±0.03 | 6.92±0.02 | 6.51±0.11 |
| Standard | 4.38±0.02 | 4.52±0.02 | 5.94±0.04 | 6.29±0.02 | 6.05±0.01 | 5.77±0.01 | 5.19±0.02 |
| HF6 | 4.46±0.02 | 4.59±0.02 | 5.89±0.03 | 6.55±0.01 | 6.40±0.01 | 6.20±0.03 | 5.70±0.01 |
| HF7 | 4.38±0.02 | 4.61±0.02 | 5.96±0.04 | 6.19±0.01 | 5.93±0.03 | 5.72±0.02 | 5.15±0.04 |
| HF8 | 4.55±0.01 | 4.62±0.01 | 5.91±0.01 | 6.60±0.04 | 6.36±0.4 | 6.35±0.01 | 5.77±0.01 |
| HF9 | 4.44±0.01 | 4.59±0.02 | 5.91±0.04 | 6.10±0.01 | 5.89±0.03 | 5.70±0.02 | 5.09±0.01 |
| HF10 | 4.51±0.02 | 4.65±0.02 | 5.94±0.03 | 6.31±0.01 | 6.05±0.01 | 5.80±0.03 | 5.22±0.01 |
| HF11 | 4.44±0.02 | 4.48±0.02 | 5.87±0.03 | 6.24±0.01 | 5.96±0.01 | 5.74±0.02 | 5.13±0.01 |
| Mean±SD | 4.45±0.05 | 4.59±0.05 | 5.92±0.04 | 6.48±0.45 | 6.29±0.56 | 6.03±0.41 | 5.47±0.46 |
| SEM | 0.097 | 0.126 | 0.111 | 0.079 | 0.102 | 0.079 | 0.065 |
| p-value | <0.0001*** | <0.0001*** | <0.00001*** | <0.000001*** | <0.0001*** | <0.000001*** | 0.002*** |

SD: Standard deviation, NS: No significant value (*<0.05; **<0.01; ***<0.001)

**Table 7: Minimum inhibitory concentration values for the finished pyrazoline compounds (HF6–11)**

| **Compounds** | **Gram-positive bacteria** | | | | **Gram-negative bacteria** | | | | **Fungi** | |
|---|---|---|---|---|---|---|---|---|---|---|
| | ***Staphylococcus aureus*** | | ***Streptococcus pyogenes*** | | ***Escherichia coli*** | | ***Pseudomonas aeruginosa*** | | ***Candida albicans*** | |
| | **MBC** | **MIC** | **MBC** | **MIC** | **MBC** | **MIC** | **MBC** | **MIC** | **MBC** | **MIC** |
| | **Conc.(mcg/mL)** | | | | | | | | | |
| Amoxicillin | 512 | 256 | 256 | 128 | 1024 | 512 | 512 | 256 | - | - |
| Ciprofloxacin | 128 | 64 | 128 | 64 | 256 | 128 | 512 | 256 | - | - |
| Fluconazole | - | - | - | - | - | - | - | - | 128 | 64 |
| Dimethyl sulfoxide | as a solvent and control | | | | | | | | | |
| HF6 | 512 | 256 | 256 | 128 | 1024 | 512 | 512 | 256 | 1024 | 512 |
| HF7 | 128 | 64 | 256 | 128 | 512 | 256 | 256 | 128 | 512 | 256 |
| HF8 | 128 | 64 | 128 | 64 | 512 | 256 | 512 | 256 | 1024 | 512 |
| HF9 | 256 | 128 | 128 | 64 | 512 | 256 | 256 | 128 | 512 | 256 |
| HF10 | 256 | 128 | 256 | 128 | 1024 | 512 | 128 | 64 | 256 | 128 |
| HF11 | 128 | 64 | 256 | 128 | 512 | 256 | 128 | 64 | 256 | 128 |

MBC: Minimum bactericidal concentration, MIC: Minimum inhibitory concentration

**Table 8: The inhibition zone of novel pyrazoline compounds (HF6–11)**

| **Compounds** | **Inhibition Zone in mm*** ** | | | | |
|---|---|---|---|---|---|
| | **Gram (+)** | | **Gram (-)** | | ***Candida albicans*** |
| | ***Staphylococcus aureus*** | ***Streptococcus pyogenes*** | ***Escherichia coli*** | ***Pseudomonas aeruginosa*** | |
| Amoxicillin* | 24 | 28 | 24 | 20 | - |
| Ciprofloxacin* | 31 | 32 | 29 | 29 | - |
| Fluconazole** | - | - | - | - | 30 |
| Dimethyl sulfoxide | 0 | 0 | 0 | 0 | 0 |
| HF6 | 20 | 20 | 17 | 24 | 27 |
| HF7 | 21 | 31 | 23 | 23 | 28 |
| HF8 | 22 | 27 | 25 | 21 | 24 |
| HF9 | 19 | 30 | 23 | 24 | 25 |
| HF10 | 24 | 27 | 23 | 25 | 26 |
| HF11 | 25 | 24 | 22 | 23 | 22 |

*Ciprofloxacin and amoxicillin are the standards for antibacterial activity

**The standard used to measure antifungal activity is fluconazole.

***When the substance's inhibition zone is between 5 and 10 mm, it is considered moderately active; when it is between 10 and 20 mm, it is considered considerably active; and when it is more than 20 mm, it is considered significantly active [35]

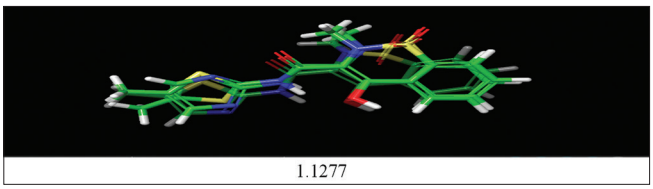


**Fig. 12: Root mean square deviation values determined for the 4m11 protein-prepared ligands**

compounds exhibit an increase starting from the 2-h mark to 4 h, with peaking around 2 h [33]. The mean±SD values during this period are approximately 6.48±0.45, 6.29±0.56, and 6.03±0.41, respectively.

Paw edema was significantly reduced by compounds HF (6–11) in comparison to the impact of propylene glycol 50%v/v (control group).

The examined chemicals (HF6-HF11) and the standard show no discernible difference at the 0-, 0.5-, and 1-h time intervals. Their

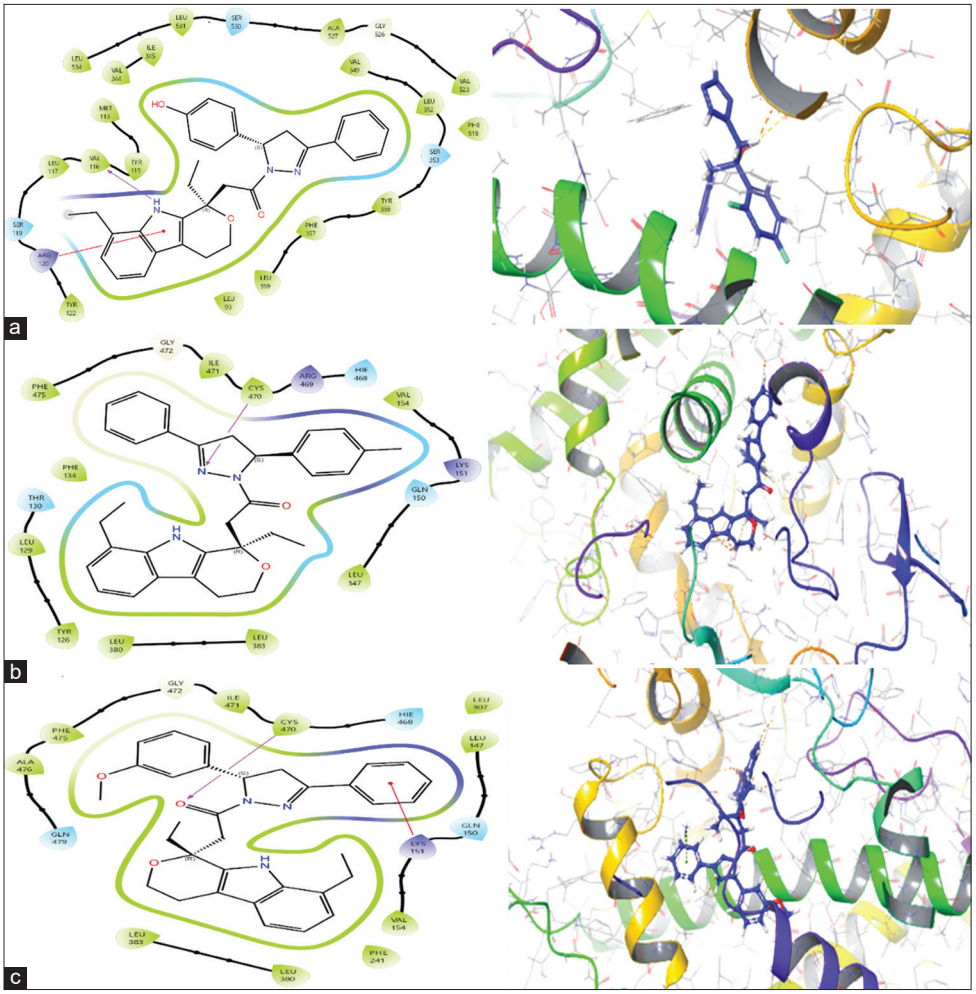


**Fig. 13: Standard and Highest Score Docked Ligands with 4MWZ. (a) Fluconazole (standard), (b) Derivative HF6, (c) Derivative HF9**

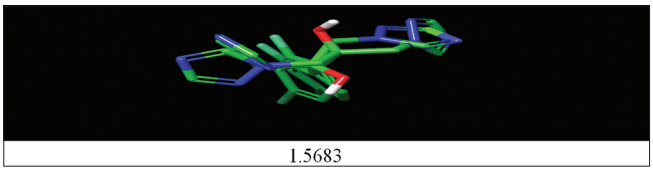


**Fig. 14: Root mean square deviation values determined for the 4WMZ protein-prepared ligands**

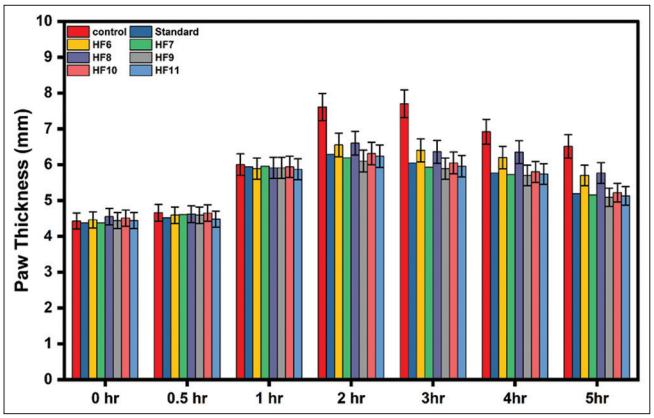


**Fig. 15: The histogram of six compounds (HF6, HF7, HF8, HF9, HF10, HF11, and control with standard), time intervals ranging from 0 to 5 h**

replacement with electron-withdrawing and/or donating groups, however, resulted in a significant activity and a large drop in paw thickness after 2–5 h, which was equivalent to the standard and control [34].

When it comes to lowering paw thickness, compounds HF7 and HF9 have a little stronger impact than the normal effect. The compounds HF10 and HF11 exhibit a comparable effect in the reduction of paw thickness, as demonstrated by the standard.

### Antimicrobial biological study

The antibacterial efficacy of the end products (HF6–11) was assessed against Gram-positive and Gram-negative bacteria, as well as fungi, using the well diffusion method. Table 7 provides the MBC and MIC values for these pyrazoline compounds alongside the reference compounds. For example, HF7, HF8, and HF11 have a MIC of 64 mcg/mL against *S. aureus*. In comparison to the reference compounds, compounds HF10 and HF11 show significant MIC values of 64 mcg/mL against *P. aeruginosa* and an MBC of 128 mcg/mL against *S. pyogenes*. Derivatives HF8 and HF9 also show noteworthy MIC values of 64 mcg/mL. In addition, out of all the chemicals tested, HF10 and HF11 were the most effective against *C. albicans*. Table 8 shows that the majority of these composites are quite active, with inhibition zones larger than 20 mm.

## CONCLUSION

Conventional organic synthesis methods were utilized to successfully produce the target compounds with satisfactory yields. ATR-FTIR and $^{1}$HNMR spectroscopy were employed to confirm the structures of six newly synthesized compounds, labeled HF6–HF11. When compared

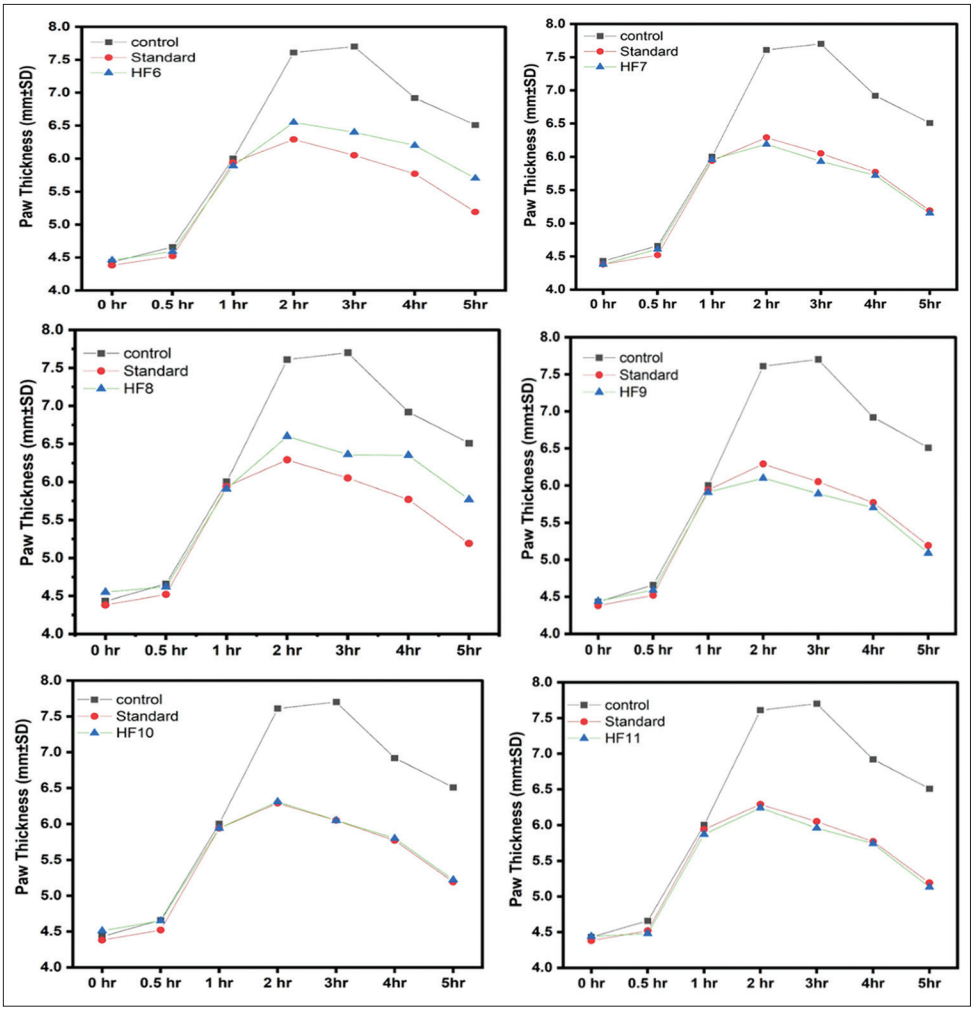


**Fig. 16: Each compound from HF6 to HF11 and (control with standard), depending on the times from 0 h to 5 h**

with diclofenac and the original drug (etodolac), the molecular docking analysis reveals encouraging results and provides a high docking score for all freshly developed compounds, with the exception of the HF10 compound when it comes to the 4m11 protein (which serves as an anti-inflammatory target). However, the docking findings of the 4WMZ protein were significantly greater than the result of fluconazole. The pharmacokinetic properties of the compounds were deemed acceptable, as demonstrated by the simulated ADME investigations. The unique pyrazoline analogs of etodolac, an NSAID, demonstrated significant anti-inflammatory properties, often matching or even exceeding the original drug's effectiveness. This was seen in experiments using live rats and the egg white-induced paw edema paradigm.

In light of the results from the preliminary microbiological assessment. The compounds' inhibitory zones showed a range of antibacterial activity from mild to strong. The zone of inhibition data and MIC values indicate that compound HF8 is more active against *S. aureus* and *S. pyogenes* than the other compounds, with a MIC of 64 mcg/mL and an MBC of 128 mcg/mL. In addition, with a MIC of 64 mcg/mL and an MBC of 128 mcg/mL, HF10 and HF11 show greater effectiveness against *P. aeruginosa*. Cytotoxicity tests will be used in future research to ascertain these drugs' selectivity index.

## ACKNOWLEDGMENT

The authors acknowledge that they have not received any funds from any organization; however, they are grateful to the College of Pharmacy at the University of Baghdad.

## CONFLICTS OF INTEREST

The authors of this study declare that they have no financial conflicts of interest or affiliations that may have influenced their work.

## FUNDING

No particular grant from a governmental, private, or non-profit funding organization was obtained for this research.

## ETHICAL STATEMENTS

The current study did not use any clinical trials, according to the authors. According to the authors, no human or human tissue experiments were conducted for this study.

## AUTHORS CONTRIBUTION

Both authors organized the research project, and the research strategy was used realistically for the synthesis of target compounds, the results of which were examined using FTIR and $^{1}$HNMR tests. The results will be evaluated and discussed, in addition to doing antimicrobial and anti-inflammatory tests. Both of the authors reviewed the study paper in detail, paying particular attention to linguistic and scientific formulation.

## REFERENCES

1. Ma Y, Frutos-Beltrán E, Kang D, Pannecouque C, De Clercq E, Menéndez-Arias L, *et al*. Medicinal chemistry strategies for discovering antivirals effective against drug-resistant viruses. Chem Soc Rev.

2021;50(7):4514-40. doi: 10.1039/d0cs01084g, PMID 33595031
2. Blanco-González A, Cabezón A, Seco-González A, Conde-Torres D, Antelo-Riveiro P, Piñeiro Á, *et al*. The role of AI in drug discovery: Challenges, opportunities, and strategies. Pharmaceuticals (Basel). 2023;16(6):891. doi: 10.3390/ph16060891, PMID 37375838
3. Ballante F, Kooistra AJ, Kampen S, De Graaf C, Carlsson J. Structure-based virtual screening for ligands of G protein-coupled receptors: What can molecular docking do for you? Pharmacol Rev. 2021;73(4):527-65. doi: 10.1124/pharmrev.120.000246, PMID 34907092
4. Salah S, Mahmoud AA, Kamel AO. Etodolac transdermal cubosomes for the treatment of rheumatoid arthritis: *Ex vivo* permeation and *in vivo* pharmacokinetic studies. Drug Deliv. 2017;24(1):846-56. doi: 10.1080/10717544.2017.1326539, PMID 28535740
5. Tziona P, Theodosis-Nobelos P, Papagiouvannis G, Petrou A, Drouza C, Rekka EA. Enhancement of the anti-inflammatory activity of NSAIDs by their conjugation with 3,4,5-trimethoxybenzyl alcohol. Molecules. 2022;27(7):2104. doi: 10.3390/molecules27072104, PMID 35408503
6. Ahmadi M, Bekeschus S, Weltmann KD, Von Woedtke T, Wende K. Non-steroidal anti-inflammatory drugs: Recent advances in the use of synthetic COX-2 inhibitors. RSC Med Chem. 2022;13(5):471-96. doi: 10.1039/d1md00280e, PMID 35685617
7. Hamdoon YS, Hadi MK. Molecular docking, ADMET, synthesis and evaluation of new indomethacin hydrazide derivatives as antibacterial agents. Pharmacia. 2024;71:1-10. doi: 10.3897/pharmacia.71.e127784
8. Shaik A, Rao AT, Venkatarao DV, Rao SV, Kishore PV. Novel etodolac-based 1,2,4-triazole derivatives as antimicrobial agents: Synthesis, biological evaluation, and molecular docking study. Russ J Org Chem. 2020;56(12):2179-87. doi: 10.1134/s1070428020120210
9. Rabee NW, Tagreed NA. Molecular docking, ADMET study, synthesis, anti-inflammatory, and antimicrobial screening of new NSAIDs conjugated with gabapentin. Iraqi J Pharm Sci. 2025;33((4SI)):362-82. doi: 10.31351/vol33iss(4si)pp362-382
10. Mervat Mohammed K, Tagreed NA. Synthesis, characterization, anti-inflammatory, and antimicrobial evaluation of new 2-pyrazolines derivatives derived from guaiacol. Iraqi J Pharm Sci. 2023;32 Suppl:254-61. doi: 10.31351/vol32isssuppl.pp254-261
11. Singh G, Goyal A, Bhatti RS, Arora S. Pyrazoline as a medicinal scaffold. Rev Bionatura. 2019;4(4):994-9. doi: 10.21931/rb/2019.04.04.10
12. Poorni KE, Gohulavani G, Muralidharan VP. Synthesis, characterization, antimicrobial and antioxidant activities of substituted pyrazolines from 2-acetylfluorene based chalcone. Int J Appl Pharm. 2022;14:111-5. doi: 10.22159/ijap.2022.v14ti.17
13. Cherfi M, Harit T, Amanchar M, Oulous A, Malek F. An overview of pyrazole-tetrazole-based hybrid compounds: Synthesis methods, biological activities and energetic properties. Organics. 2024;5(4): 575-97. doi: 10.3390/org5040030
14. Jain SK, Singhal R. A review on pyrazoline derivatives as antimicrobial agent. Int J Pharm Pharm Sci. 2020;12(6):15-24. doi: 10.22159/ijpps.2020v12i6.37456
15. Shaymaa Kanaan K, Omar TN. Synthesis and preliminary anti-inflammatory and anti-microbial evaluation of new 4,5-dihydro-1H-pyrazole derivatives. Iraqi J Pharm Sci. 2023;32 Suppl:262-70. doi: 10.31351/vol32isssuppl.pp262-270
16. Lominoga ER, Zadorozhnii PV, Kobets VV, Kiselev VV, Kharchenko AV. Synthesis, spectral characteristics, and molecular docking studies of 2-(2,4-dichlorophenoxy)-N-(2,2,2-trichloro-1-(3-arylthioureido)ethyl) acetamide. Eng Proc. 2023;56(1):195. doi: 10.3390/asec2023-15324
17. Sharma D, Kumar S, Narasimhan B, Ramasamy K, Lim SM, Shah SA, *et al*. 4-(4-bromophenyl)-thiazol-2-amine derivatives: Synthesis, biological activity and molecular docking study with ADME profile. BMC Chem. 2019;13(1):60. doi: 10.1186/s13065-019-0575-x, PMID 31384808
18. Ali RH, Al-Hamashi AA. Design, synthesis, and preliminary antiproliferative evaluation of 1,2,4-thiadiazole derivatives as possible histone deacetylase inhibitors. Iraqi J Pharm Sci. 2025;33((4SI)):57-66. doi: 10.31351/vol33iss(4SI)pp57-66
19. Mohammed M, Amjed Adnan A. *In-silico* design, molecular docking, molecular dynamic simulations, molecular mechanics with generalised born and surface area solvation study, and pharmacokinetic prediction of novel diclofenac as anti-inflammatory compounds. Turk Comp Theor Chem. 2024;8(3):108-21. doi: 10.33435/tcandtc.1355772
20. Maurya AK, Mishra N. *In silico* validation of coumarin derivatives as potential inhibitors against Main protease, NSP10/NSP16-Methyltransferase, Phosphatase and Endoribonuclease of SARS CoV-2. J Biomol Struct Dyn. 2021;39(18):7306-21. doi: 10.1080/07391102.2020.1808075, PMID 32835632
21. Shridhar Deshpande N, Mahendra GS, Aggarwal NN, Gatphoh BF, Revanasiddappa BC. *Insilico* design, ADMET screening, MM-GBSA binding free energy of novel 1,3,4 oxadiazoles linked Schiff bases as PARP-1 inhibitors targeting breast cancer. Future J Pharm Sci. 2021;7(1):174. doi: 10.1186/s43094-021-00321-4
22. Hamad AA, Omer RA, Kaka KN, Amin AA, Ahmed KM, Rashid RF, *et al*. A review: New synthesis of chalcone derivatives and their applications. Chem Rev Lett. 2025;8:329-51. doi: 10.22034/crl.2025.480229.1427
23. Al-Nakeeb MR, Omar TN. Synthesis, characterization and preliminary study of the anti-inflammatory activity of new pyrazoline containing ibuprofen derivatives. Iraqi J Pharm Sci. 2019;28(1):131-7. doi: 10.31351/vol28iss1pp131-137
24. Hassan OM, Sarsam SW. Synthesis, characterization and preliminary anti-inflammatory evaluation of new etodolac derivatives. Iraqi J Pharm Sci. 2019;28(1):106-12. doi: 10.31351/vol28iss1pp106-112
25. Hadi MK, Abdulkadir MQ, Abdul-Wahab A. Synthesis and antimicrobial evaluation of sulfonylhydrazide derivatives of etodolac. Int J Drug Deliv Technol. 2021;11(3):1000-3. doi: 10.25258/ijddt.11.3.59
26. Mahdi MF, Raauf AM, Mohammed NM. Synthesis, characterization and preliminary pharmacological evaluation of new non-steroidal anti-inflammatory pyrazoline derivatives. Eur J Chem. 2015;6(4):461-7. doi: 10.5155/eurjchem.6.4.461-467.1321
27. Mahdi GA, Dakhel ZA. Synthesis, characterization, and initial pharmacological assessment of new naproxen with 1,3,4-thiadiazol-2-amine derivatives. Gomal J Med Sci. 2024;22(3):252-61. doi: 10.46903/gjms/22.03.1675
28. Abdulhamza HM, Farhan MS. Synthesis, characterization and preliminary anti-inflammatory evaluation of new fenoprofen hydrazone derivatives. Iraqi J Pharm Sci. 2020;29(2):239-44. doi: 10.31351/vol29iss2pp239-244
29. Castro-Alvarez A, Costa AM, Vilarrasa J. The performance of several docking programs at reproducing protein-macrolide-like crystal structures. Molecules. 2017;22(1):136. doi: 10.3390/molecules22010136, PMID 28106755
30. Mawla MC, Omar TN. *In-silico* molecular docking studies, synthesis and preliminary pharmacological evaluation of new pyrazoline derivatives bearing pyridine ring scaffolds. Int J Appl Pharm. 2025;17(4):309-25. doi: 10.22159/ijap.2025v17i4.54404
31. Yadav CS, Azad I, Khan AR, Nasibullah M, Ahmad N, Hansda D, *et al*. Recent advances in the synthesis of pyrazoline derivatives from chalcones as potent pharmacological agents: A comprehensive review. Results Chem. 2024;7:101326. doi: 10.1016/j.rechem.2024.101326
32. Orján EM, Kormányos ES, Fűr GM, Dombi Á, Bálint ER, Balla Z, *et al*. The anti-inflammatory effect of dimethyl trisulfide in experimental acute pancreatitis. Sci Rep. 2023;13(1):16813. doi: 10.1038/s41598-023-43692-9, PMID 37798377
33. Huang J, Chen R, Zhou J, Zhang Q, Xue C, Li Y, *et al*. Comparative pharmacokinetic study of the five anti-inflammatory active ingredients of *Inula cappa* in a normal and an LPS-induced inflammatory cell model. Front Pharmacol. 2022;13:981112. doi: 10.3389/fphar.2022.981112, PMID 36199688
34. Mohammed ZB, Omar TN. Chemical design, synthesis and biological evaluoation of mutual prodrug of gabapentin with different types of phenolic and alcoholic antioxidants. Syst Rev Pharm. 2021;12(1): 858-68.
35. Sahib HA, Mohammed MH. Synthesis and preliminary biological activity evaluation of new N-substituted phthalimide derivatives. Iraqi J Pharm Sci. 2020;29(1):247-52. doi: 10.31351/vol29iss1pp247-252